# Formation of Self-Assembled Octadecylsiloxane Monolayers on Mica and Silicon Surfaces Studied by Atomic Force Microscopy and Infrared Spectroscopy

**T. Vallant, H. Brunner, U. Mayer, and H. Hoffmann***

*Institute of Inorganic Chemistry, Vienna University of Technology, Getreidemarkt 9, A-1060 Wien, Austria*

**T. Leitner, R. Resch, and G. Friedbacher***

*Institute of Analytical Chemistry, Vienna University of Technology, Getreidemarkt 9, A-1060 Wien, Austria*

*Received: February 25, 1998; In Final Form: June 25, 1998*

The formation and growth of self-assembled octadecylsiloxane monolayers on native silicon and mica substrates have been studied using atomic force microscopy, ellipsometry, and infrared spectroscopy. Submonolayer ODS films of varying surface coverages were prepared by immersing the substrates into dilute solutions of octadecyltrichlorosilane in toluene for different periods of time, and the submonolayer film structures were compared between mica and silicon substrates for different water contents of the adsorbate solutions and for different time delays between solution preparation and substrate immersion (solution age). It was found that, in general, both a continuous growth (formation of disordered, liquidlike submonolayers) and an island-type growth (formation of organized assemblies with vertically aligned hydrocarbon chains) are involved in the formation of ODS monolayers, whereby the relative contributions depend strongly on the solution properties. With increasing water content or increasing age of the adsorbate solution, island-type growth is strongly favored on both silicon and mica surfaces, which indicates the kinetically controlled formation of larger, preordered aggregates of silanol molecules as the primary hydrolysis products in solution. For identical conditions of film preparation, both the degree of structural order in the submonolayer films and the overall adsorption rate was found to be higher on mica in comparison to silicon. The higher structural order was interpreted as a consequence of the lower hydroxyl group concentration and a correspondingly enhanced surface diffusion rate of weakly bound film molecules on a mica substrate. The enhanced adsorption rate, on the other hand, points to some additional activation of a mica surface with respect to silanol adsorption, which might be related to its ionic composition containing mobile surface charges in contrast to the covalent, neutral character of a native silicon surface.

## Introduction

Self-assembled monolayers of long-chain organosilane compounds ($R-SiCl_3$, $R-Si(OCH_3)_3$, R = alkyl group with >10 carbon atoms) on hydroxylated surfaces have been the subject of numerous investigations since their discovery by Sagiv et al.in 1980.[1−21] General agreement has emerged from those previous studies that complete monolayers of these compounds represent highly ordered, crystalline-like phases in which the hydrocarbon chains are oriented close to perpendicular to the surface on a variety of different substrates including native silicon ($Si/SiO_2$),[3−9] mica,[10−12] germanium,[13−15] zinc selenide,[13,14] glass,[16,17] alumina,[4,9,18,19] and gold.[20,21] The mechanism for nucleation and growth of these films, however, remains a matter of controversy. A continuous growth model has been derived from X-ray reflectivity[22] and IR-ATR[23,24] data, which indicate that a liquidlike, disordered film is formed initially, which is successively converted into the final, highly ordered film structure with increasing coverage. In contrast, AFM studies[11] and X-ray diffraction results[25] provide evidence that submonolayer films are composed of islands of densely packed film molecules with a local structure similar to the complete monolayer, which are separated by uncovered surface regions. With increasing coverage, these islands have been shown to grow laterally and combine under formation of larger aggregates until a complete monolayer is formed.[11] In this controversy between a continuous growth and an island-type growth mechanism, little attention has been paid, so far, to the specific conditions of film preparation, such as the water content of the adsorbate solution, the solvent, the precursor concentration, or the type and pretreatment of the substrate. As long as a certain minimum concentration of surface water is present, these parameters seem to have little influence on the properties of *complete* monolayers and therefore vary, in general, substantially between different studies. It seems plausible, however, that the structure of *incomplete* (submonolayer) films depends strongly on some of these parameters. For example, Grunze et al.[26] have shown in a recent AFM study that the shape and size of submonolayer islands deposited on a Si(100) substrate from dilute octadecyltrichlorosilane (OTS) solutions differ significantly between a dry cleanroom environment and normal laboratory conditions during the film preparation, even though the final monolayer films are indistinguishable. This was ascribed to the influence of the water concentration at the substrate surface on the rate of surface polymerization and surface diffusion of the film molecules. On the basis of these findings, it might be expected that the size of the primary islands deposited on the substrate also depends on the degree of polymerization of silanol precursors in the adsorbate solution, which, in turn, depends on a variety of factors including the water content, the reaction time, or the type of solvent. Additionally, if one considers solution polymerization and film adsorption as two competing reactions,[27] the type of substrate

S1089-5647(98)01282-6 CCC: $15.00 
Published on Web 08/21/1998

and, in particular, the surface concentration of hydroxyl groups, which serve as nucleation centers and anchor points in the film-formation process, might have a pronounced influence on the growth process and on the submonolayer film structure. Thus, conflicting results about island-type versus continuous film growth in previous studies might simply originate in different substrate properties and/or different experimental parameters used for film preparation.

The primary goal of the present study was, therefore, to investigate the influence of the substrate and the specific preparation conditions on the structure of submonolayer films and on the film growth mechanism. For this purpose, we have used two largely different substrates—native silicon ($Si/SiO_2$) and mica—and have followed the growth process of octadecylsiloxane (ODS) monolayers under systematic variation of the water content in the adsorbate solution and of the solution age (i.e., the time between solution preparation and immersion of the substrate) with all other parameters (pretreatment of the substrates, adsorbate concentration, solvent, surrounding atmosphere) kept constant in these experiments. Silicon and mica have been chosen because they are the two most commonly used substrates for this type of monolayers and also represent two extreme cases with respect to the surface OH-group concentration: On native silicon, a hydroxyl group coverage up to $5 \times 10^{14}/cm^{-2}$ can be achieved at room temperature,[22] which approximately equals the packing density of the film molecules in a complete monolayer film,[7] whereas mica is known to possess very few, if any, surface OH groups[28] and the film molecules are believed to be primarily physisorbed and/or H-bonded on the substrate surface.

## Experimental Section

**Compounds, Solvents, and Substrates.** Octadecyltrichlorosilane (Aldrich, 95%), toluene (Aldrich, 99.8%), acetone (Aldrich, 99.9%), and ethanol (Austria Hefe AG, 99.8%) were commercially available and used as received. P-doped, (100)-oriented, and single-sided polished silicon wafers (Wacker Chemitronic, test grade, 14−30 Ω cm resistivity, 0.5 mm thickness) were cut into pieces of appropriate size ($25 \times 18$ $mm^2$ for IR measurements, $12 \times 12$ $mm^2$ for AFM measurements) and cleaned by ultrasonic treatment in toluene, rinsing with acetone and ethanol and blow-drying in high-purity nitrogen followed by a 15 min exposure to a UV/ozone atmosphere in a commercial cleaning chamber (Boekel Industries, model UVClean) equipped with a low-pressure mercury quarz lamp ($\lambda_{max} = 185$ and 254 nm). This treatment yields a hydrophilic, contamination-free surface with a native oxide layer of 12−14 Å thickness, as routinely checked by ellipsometry. Sheets of muscovite mica (Structure Probe Inc.) were cut into pieces of appropriate size ($30 \times 20$ $mm^2$ for IR-spectroscopy, $12 \times 12$ $mm^2$ for AFM measurements) and cleaved just prior to film adsorption using an adhesive tape.

**Preparation of the Adsorbate Films.** The preparation of the adsorbate solutions and the film adsorption was carried out in a glovebox purged with dry nitrogen to exclude any influences of water vapor in the surrounding atmosphere. Octadecylsiloxane (ODS) films on silicon and mica were prepared by immersing the substrates for certain periods of times in dilute solutions of octadecyltrichlorosilane in toluene ($c = 5 \times 10^{-4}$ mol/L) with a preset water concentration, which was obtained by mixing appropriate amounts of anhydrous and water-saturated solvent. The water content of the adsorbate solutions was determined by Karl Fischer titration. The film-covered substrates were cleaned by rinsing with toluene, acetone, and ethanol and finally blow-dried with nitrogen. On silicon, the film thickness was routinely measured by ellipsometry immediately after film adsorption. To estimate the effect of a quasi-Langmuir−Blodgett deposition upon removal of the substrate from the adsorbate solution, a "multiple dip" experiment as described by Schwartz et al.[29] was performed: A silicon substrate was quickly immersed and removed 4 times in a 0.5 mmol/L OTS solution with a water content of 12 mmol/L (total immersion time ∼ 8 s), after which a film thickness of 6.7 Å was measured ellipsometrically. A second substrate was immersed for 18 s in the same solution (one dip), resulting in a film thickness of 12.2 Å. Assuming an approximately linear film growth in this low-coverage regime ($\Theta \propto t$), a surface coverage increase per second is essentially identical for the multiple-dip and the one-dip sample, and thus, a film transfer at the solution−air interface can be neglected.

**Ellipsometric Measurements.** Ellipsometric film thickness measurements were carried out on a Plasmos SD 2300 ellipsometer with a rotating analyzer and a He−Ne laser ($\lambda = 632.8$ nm) at 68° incidence as the light source. The ellipsometric angles (relative phase shift $\Delta$ and amplitude ratio $\Psi$) were converted into film thicknesses using the commercial instrument software which is based on the McCrackin algorithm.[30] An isotropic three-phase model ($Si/SiO_2$/air) was used for the substrate and a four-phase model ($Si/SiO_2$/adsorbate/air) for the sample. A measurement of the clean reference $Si/SiO_2$ yielded the thickness of the native oxide layer using literature values[31] for the optical constants of Si ($n = 3.865$, $k = 0.020$) and $SiO_2$ ($n = 1.465$, $k = 0$). Subsequent measurement of the film-covered substrate and substitution of the substrate parameters together with assumed values for the adsorbate ($n = 1.50$ and $k = 0$) into the four-phase model allowed the calculation of the adsorbate layer thickness.[32] Submonolayer coverages of ODS films were determined by dividing the ellipsometrically measured thickness by the thickness of a complete ODS monolayer for which a value of 26.5 Å, in close agreement to the reported literature data,[4,5,7,9] was repeatedly obtained in this study regardless of the specific film preparation conditions.

**FTIR Spectroscopy.** FTIR spectra were measured with a Mattson RS2 FT-IR spectrometer equipped with a narrow-band MCT detector. For external reflection measurements with silicon substrates, the samples where mounted in a custom-made reflection unit, which is described in detail elsewhere.[33] P-polarized radiation at an incidence angle of 80° was used. IR transmission spectra with mica substrates were measured using a commercial variable-angle transmission unit (Harrick) equipped with a Brewster-angle polarizer. To minimize interference fringes in the transmission spectra due to multiple reflections at the sample/air interfaces, p-polarized radiation at 56° incidence (Brewster angle of mica) was used.[34] Additionally, even minor thickness variations between sample and reference as well as their different orientation in the spectrometer had to be carefully avoided[34] by using the same substrate for both the background and the sample spectrum. With the film preparation procedure described above, both sides of the substrate were covered with the adsorbate and the effective film thickness for a transmission spectrum was, therefore, twice the thickness for a reflection spectrum, where only the front surface is probed by the IR radiation. For each spectrum, 1024 (external reflection) or 256 scans (transmission) at 4 $cm^{-1}$ resolution were averaged from the film-covered substrate and the clean reference surface. The interferograms were apodized using a triangular function and zero-filled to yield spectra with one data point per wavenumber. A linear baseline correction was applied to the

raw spectra in order to remove baseline offsets and slopes due to spectrometer instabilities and/or irreproducible mounting of sample and reference.

**AFM Measurements.** AFM measurements were carried out with a NanoScope III AFM (Digital Instruments, Santa Babara, CA) operated in tapping mode. All measurements were perfomed in air using commercial silicon cantilevers with typical spring constants of 13−100 N/m and a resonance frequency of approximately 300 kHz in air. Data analysis was performed with the NanoScope III software. The height distributions of the submonolayer islands were determined from cross-sectional profiles at several random locations of each AFM image and from height histograms obtained with the Nansoscope III software from three-dimensional height profiles of the submonolayer films. The average thickness of a submonolayer film was obtained as the ratio of the film volume, which was calculated from the three-dimensional AFM height profile, and the geometrical surface area. The surface coverage was calculated as the ratio of these values and the thickness of a complete ODS monolayer in analogy to the ellipsometric data. Good agreement was found between these values and the surface coverages determined by a Nanoscope III software option, which calculates the ratio between the occupied area of surface species above a certain height threshold and the total geometrical area of the substrate surface.

**IR Spectra Simulations.** Both reflection and transmission IR spectra of ODS films on silicon and mica were calculated using a semiempirical matrix method described in detail elsewhere.[8] Briefly, the spectral simulations in this study are based on a classical three-phase model for external reflection spectra (air/adsorbate/substrate) and a five-phase model for transmission spectra (air/adsorbate/substrate/ adsorbate/air) with parallel phase boundaries. Each phase is characterized by its thickness $d_i$ and its dielectric function $\epsilon_i(\nu,\xi) = (n_i(\nu,\xi) + jk_i(\nu,\xi))^2$ ($n_i$ = refractive index, $k_i$ = absorption coefficient), which, in general, is a second-rank tensor and depends on both frequency $\nu$ and direction $\xi$. Air, silicon, and mica were treated as optically isotropic (direction independent) and nonabsorbing ($k = 0$) with a frequency-independent refractive index ($n_{air} = 1$, $n_{Si} = 3.42$,[35] $n_{mica} = 1.45$[36]) in the wavenumber range of interest for the present study (CH stretching region). The dielectric functions of the ODS submonolayer films were constructed, as previously described, from IR spectra of appropriate octadecyl reference compounds,[7,8] assuming a heterogeneous film structure consisting of ordered, densely packed domains identical to the full ODS monolayer structure (8° tilt angle between the hydrocarbon chain axes and the surface normal[8]) together with liquidlike, disordered regions with a completely isotropic orientation of the film molecules. For the thickness of the adsorbate layer, either the ellipsometrically measured film thicknesses (on silicon) or the indirectly derived values from the AFM images (on mica) were used. Thus, the only fitting parameter in the simulation procedure for both reflection and transmission spectra was the weighting factor between ordered and disordered film domains. Using the above parameters, the amplitudes of the electric field reflected and transmitted by the sample can be calculated and the simulated IR reflection or transmission spectrum is finally obtained as the square of the corresponding Fresnel coefficients.

## Results and Discussion

**1. Influence of the Water Content of the Adsorbate Solution. 1.1. ODS Films on Native Silicon Surfaces (Si/SiO$_2$).** Figure 1 shows two series of AFM images of submonolayer ODS films on native silicon for different adsorption times and two different water concentrations (A, 4.5 mmol/L; B, 12.8 mmol/L) of the adsorbate solutions. The time between solution preparation and immersion of the substrate was kept constant at 1 h in these experiments (see section 2). Two immediate differences in the film growth process between these two series are apparent in these pictures: For the higher water concentration (series B), both the surface coverage for a given adsorption time and the average island sizes are significantly larger (note the different time scales for series A and B in Figure 1). In Table 1, the ellipsometrically measured thicknesses of these submonolayer films $d_{ell}$ are listed together with the corresponding surface coverages $\Theta_{ell}$, and these values are compared to the corresponding data $d_{AFM}$ and $\Theta_{AFM}$ derived from AFM measurements (see Experimental Section), which are also included in Table 1. In general, good agreement is obtained between these two sets of data derived from different methods, whereby significant deviations are observed only for the lowest

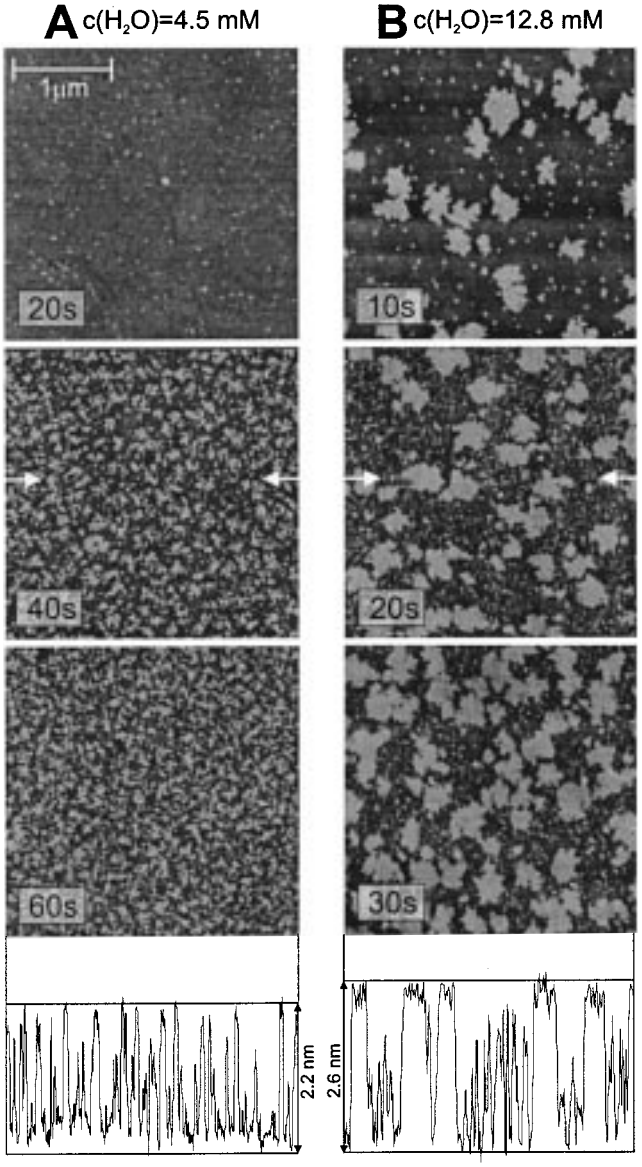


**Figure 1.** AFM images of submonolayer ODS films on native silicon substrates as a function of the time of adsorption for two different water contents of the adsorbate solutions (A, 4.5 mmol/L; B, 12.8 mmol/L). The solution age for each sample was 1 h. The height profiles in the lower part were measured along the horizontal lines marked by white arrows in the middle image of each series.

**TABLE 1: Mean Film Thicknesses and Surface Coverages Determined by Ellipsometry ($d_{ell}$, $\Theta_{ell}$) and Atomic Force Microscopy ($d_{AFM}$, $\Theta_{AFM}$) of Submonolayer ODS Films Prepared on Native Silicon Substrates from 0.5 mmol/L Solutions of OTS in Toluene with Different Water Concentrations ($c_{H_2O}$) and Different Substrate Immersion Times ($t$)[a]**

| $t$ (s) | $c_{H_2O}$ (mmol/L) | $d_{ell}$ (Å) | $\Theta_{ell}$ (%) | $d_{AFM}$ (Å) | $\Theta_{AFM}$ (%) | $\Theta_{po}$ (%) | $\Theta_{pd}$ (%) |
|---|---|---|---|---|---|---|---|
| 20 | 4.5 | 5.8 ± 0.2 | 22 ± 0.8 | 3.2 ± 1.1 | 12 ± 4 | 0 | (22)[b] |
| 40 | 4.5 | 12.1 ± 0.2 | 46 ± 0.8 | 11.9 ± 0.5 | 45 ± 2 | 8 ± 4 | 38 ± 3 |
| 60 | 4.5 | 15.2 ± 0.1 | 57 ± 0.4 | 14.9 ± 0.5 | 56 ± 2 | 23 ± 2 | 34 ± 2 |
| 10 | 12.8 | 12.3 ± 0.2 | 46 ± 0.8 | 10.4 ± 0.5 | 39 ± 2 | 19 ± 2 | (27)[b] |
| 20 | 12.8 | 17.4 ± 0.3 | 66 ± 1.2 | 16.4 ± 0.5 | 62 ± 2 | 34 ± 2 | 32 ± 2 |
| 30 | 12.8 | 19.7 ± 0.1 | 74 ± 0.4 | 19.4 ± 0.5 | 73 ± 2 | 45 ± 3 | 29 ± 3 |

[a] The AFM images of the corresponding samples are shown in Figure 1. The partial surface coverages of ordered ($\Theta_{po}$) and disordered ($\Theta_{pd}$) portions of the submonolayer films are based on the ellipsometrically determined total coverages $\Theta_{ell}$ and were derived from the IR reflection spectra shown in Figure 2. See text for details. [b] Systematic deviation between calculated and experimental values (see text).

surface coverages in both series (see below). These results confirm the substantial acceleration of the growth rate with increasing water concentration in the adsorbate solution, which was already visually observed in the AFM images of Figure 1. A closer look at these images and the corresponding height profiles included in Figure 1 indicates that the islands formed in series A remain uniformly small with increasing adsorption time whereas at higher water concentration (series B) two types of islands—small, dotlike features and larger, multiply branched islands—are visible from the very beginning, whereby the number density of the larger islands appears to increase more rapidly with increasing surface coverage compared to the small, dotlike islands. Additionally, the small islands in both series exhibit a random height distribution, whereas the large islands in series B show fairly constant heights ranging between 22 and 26 Å. These latter values are close to the ellipsometrically determined thickness of a complete ODS monolayer film,[4,5,7,9] which has been shown in numerous previous studies to consist of densely packed ODS molecules in an all-trans hydrocarbon chain configuration oriented close to normal to the surface.[1−9] Thus, the film growth mechanism appears to shift from a uniform growth of small, disordered aggregates at low water concentration to an island-type growth of fairly large, preordered molecule ensembles at high water concentration. This is nicely confirmed by the external reflection infrared spectra shown in Figure 2 for the same two series of samples prepared at different water concentrations of the adsorbate solution. The general characteristics of reflection infrared spectra on nonmetal substrates such as silicon have been discussed in detail in several previous publications.[8,9,16] Briefly, vibrations both parallel and perpendicular to the substrate surface can be detected on nonmetal substrates, but they appear as bands pointing in opposite directions in the reflection spectrum. As a consequence, anisotropic films with a uniform surface orientation of the film molecules generally yield fairly complex reflection spectra consisting of superimposed upward- and downward-pointing absorptions, each reflecting the particular surface orientation of the corresponding vibrational dipole moment. In isotropic films, on the other hand, the film molecules are oriented randomly on the surface and all vibrational dipoles adopt the same average surface orientation. For certain measurement conditions, a completely inverted absorption spectrum may result, as we have shown previously for a thin film of paraffin oil on a silicon surface.[8] These unique spectral characteristics can be used for a very sensitive detection of

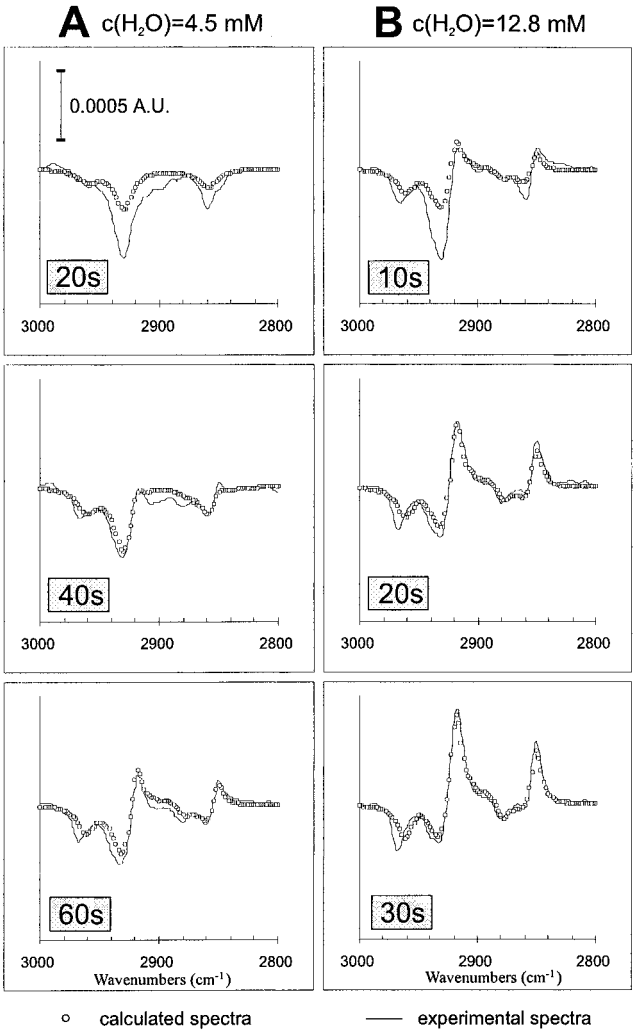


**Figure 2.** CH stretching absorptions in ERIR spectra of submonolayer ODS films on native silicon substrates as a function of the time of adsorption for two different water contents of the adsorbate solutions (A, 4.5 mmol/L; B, 12.8 mmol/L). The corresponding AFM images of each sample are shown in Figure 1.

structural order−disorder transitions caused, for example, by a decrease of the hydrocarbon chain length of the film molecules[8,37] or by a change in the surface coverage.[9,38] A very similar situation is encountered in the spectra shown in Figure 2. To a first approximation, they represent a mixture between a liquidlike, disordered hydrocarbon film with downward-pointing, broad absorption bands at 2858 ($\nu_s$ ($CH_2$)), 2928 ($\nu_{as}$ ($CH_2$)), and 2960 $cm^{-1}$ ($\nu$ ($CH_3$))[8] and a densely packed, highly ordered hydrocarbon layer with close-to-perpendicular chain axis orientation,[8,9] which gives rise to sharp absorptions at 2850 ($\nu_s$ ($CH_2$)) and 2920 $cm^{-1}$ ($\nu_{as}$ ($CH_2$)) pointing in the upward, positive direction and downward-pointing bands for the terminal methyl group at 2879 ($\nu_s$ ($CH_3$)) and 2968 $cm^{-1}$ ($\nu_{as}$ ($CH_3$)). We have attempted to fit the experimental spectra in Figure 2 with simulated spectra representing a weighted average between the above-described anisotropic and isotropic film structures (see Experimental Section). The resulting simulated sum spectra are included in Figure 2 (open circles), and the corresponding partial coverages of ordered and disordered regions $\Theta_{po}$ and $\Theta_{pd}$, which result from the total surface coverages and the weighting factors used for the simulated spectra, are included in Table 1. The agreement between the calculated and experimental spectra in Figure 2 is generally very good, except for the first low-coverage spectrum of each series, where the downward-pointing absorp-

tions representing the disordered film regions are significantly stronger than predicted by the calculations. At the moment, we do not have a satisfactory explanation for these deviations. It must be emphasized, however, that these calculations are based on the assumption that the submonolayer films consist of only two structural domains with varying relative coverages, which is probably only a crude approximation of the true film structure as a function of coverage. It seems plausible, for example, that a liquidlike, isotropic arrangement and the anisotropic, full monolayer structure represent only two extremes, between which all kinds of intermediate structures are adopted to varying extents in the course of the film growth process. An attempt to simulate this more realistic situation seems unrewarding, however, because of the large number of fitting parameters which would have to be assumed more or less arbitrarily and prevent an unambiguous result. Even with the simplistic model chosen here a clear trend can be seen in the data derived from Figure 2: In both series with different water concentration of the adsorbate solution, a disordered film structure dominates at the beginning of the growth process. With increasing total surface coverage (increasing adsorption time), this disordered submonolayer coverage $\Theta_{pd}$ goes through a maximum and decreases afterward whereas the percentage of ordered film domains $\Theta_{po}$ increases slowly in the beginning and rapidly toward the end of the monolayer growth process. The influence of the water concentration in the adsorbate solution is most clearly seen by comparing the second sample of series A with the first sample of series B, both of which have essentially the same total surface coverage of about 45%: Increasing the water concentration by about a factor of 3 reduces the adsorption time by a factor of 4 and shifts the ratio between ordered and disordered film regions from about 1:5 (series A, sample 2) to 1:1.5 (series B, sample 1). Thus, with increasing water concentration, the overall rate of adsorption increases and the equilibrium between ordered and disordered domains shifts toward the ordered film structure. Returning to the corresponding AFM images and height profiles in Figure 1, it seems plausible to assign the large islands in series B to the ordered domains and the small islands in series A to the disordered film regions. However, a comparison of the first sample in series B with the last sample in series A—which have slightly different total coverages but the same 1:1.5 ratio between ordered and disordered structures—shows that ordered film regions do exist also in submonolayer films with a small average island size.

**1.2. ODS Films on Mica Surfaces.** Contrary to silicon, mica is not suitable for ellipsometric film thickness measurements or IR reflection spectroscopy due to its low refractive index and its soft and flexible texture. A detailed analysis of the submonolayer film structures as described above is, therefore, not possible here. Thus, only two representative AFM images of submonolayer ODS films on mica prepared from solutions with different water content are shown together with the corresponding height profiles in Figure 3. These samples were prepared by immersing the substrates immediately after preparation of the adsorbate solutions, and a constant adsorption time of 20 s was used. The same qualitative trends as with a native silicon substrate are observed in Figure 3 as a function of the water concentration in solution: Both the surface coverage and the average island size increase with increasing water concentration. In a solution with 4.5 mmol of $H_2O$/L (Figure 3A), small, dotlike features similar to Figure 1A with a fairly random height distribution are visible in the AFM image, whereas for 12.8 mmol of $H_2O$/L (Figure 3B), large islands with lateral dimensions $>1$ $\mu$m and heights of about 25 Å are

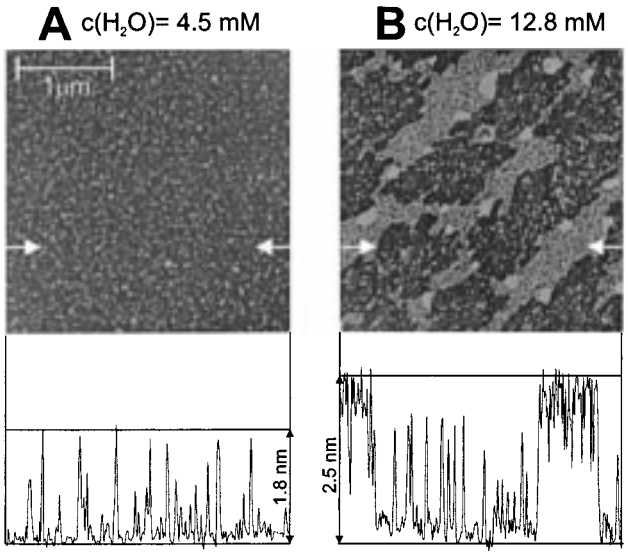


**Figure 3.** AFM images of submonolayer ODS films on mica substrates prepared by adsorption for 20 s in freshly prepared solutions with different water contents (A, 4.5 mmol/L; B, 12.8 mmol/L). The height profiles were measured along the horizontal lines marked by white arrows.

observed together with much smaller features of lower thickness. The surface coverages determined from these images were 19% (Figure 3A) and 39% (Figure 3B), i.e., the growth rate is approximately doubled upon increasing the water concentration from 4.5 to 12.8 mmol/L. The unusually large size and the directional shape of the islands in Figure 3B might be caused, in part, by the solvent rinse after removal of the sample from the adsorbate solution. Weakly bound, physisorbed islands might coalesce during this final rinsing procedure in the preferred direction of solvent drainage, whereby the lack of surface OH groups of a mica substrate, resulting in a weaker substrate−adsorbate bonding, is expected to promote this effect in comparison to silicon substrates, where islands as large as those in Figure 3B have never been observed.

**2. Influence of the Age of the Adsorbate Solution.** In Figure 4, AFM images and height profiles of submonolayer ODS films prepared from solutions of different "age" (i.e., the time between solution preparation and immersion of the substrate) with a constant immersion time of 20 s are shown on native silicon (Figure 4A) and mica substrates (Figure 4B). The first image on each substrate was obtained with a freshly prepared OTS solution, and for the second image, the solution was prepared 2 h before immersion of the substrate and stored in a sealed vessel. In Table 2, the corresponding mean film thicknesses and surface coverages determined by ellipsometry and AFM are listed. Qualitatively, the solution age seems to have a similar effect on the film growth process as the water concentration of the solution: In the "old" solution, the adsorption is significantly faster on both silicon and mica substrates and also the average island size is somewhat larger compared to the freshly prepared solution, although this latter effect is not as pronounced here as in Figures 1 and 3 for different water concentrations and also the island heights in Figure 4 do not reach the limiting value of about 26 Å as in Figures 1B and 3B. The last two columns in Table 2 list, again, the partial surface coverages of ordered and disordered domains $\Theta_{po}$ and $\Theta_{pd}$ in the submonolayer films on silicon and mica, which were derived from the infrared spectra shown in Figure 5. Because of the low total surface coverages resulting in the freshly prepared adsorbate solutions, only the samples from the

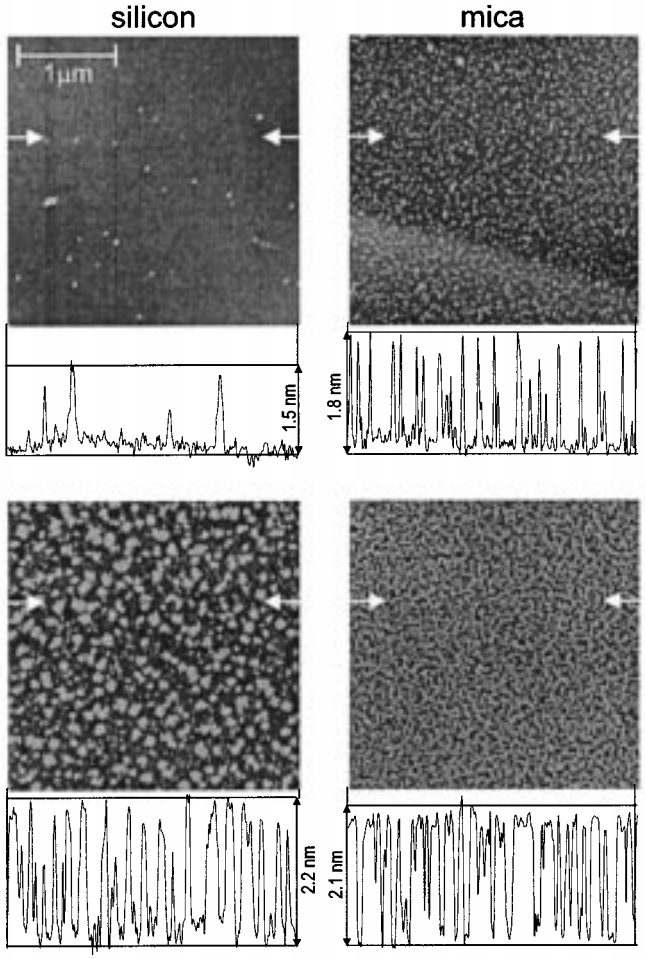


**Figure 4.** AFM images of submonolayer ODS films on native silicon and mica substrates prepared by substrate immersion for 20 s immediately after solution preparation (top images) and 2 h after solution preparation (bottom images). The water content of the adsorbate solutions was 4.5 mmol/L. The height profiles were measured along the horizontal lines marked by white arrows in each image.

**TABLE 2: Mean Film Thicknesses and Surface Coverages Determined by Ellipsometry ($d_{ell}$, $\Theta_{ell}$) and Atomic Force Microscopy ($d_{AFM}$, $\Theta_{AFM}$) of Submonolayer ODS Films on Native Silicon and Mica Substrates Prepared by 20 s Immersion in 0.5 mmol/L Solutions of OTS in Toluene ($c_{H_2O}$ = 4.5 mmol/L)[a]**

| substrate | solution age (h) | $d_{ell}$ (Å) | $\Theta_{ell}$ (%) | $d_{AFM}$ (Å) | $\Theta_{AFM}$ (%) | $\Theta_{po}$ (%) | $\Theta_{pd}$ (%) |
|---|---|---|---|---|---|---|---|
| silicon | 0 | 1.1 ± 0.1 | 4 ± 0.4 | 1.0 ± 0.3 | 4 ± 1 | *c* | *c* |
| mica | 0 | *b* | *b* | 6.0 ± 0.8 | 23 ± 3 | *c* | *c* |
| silicon | 2 | 13.9 ± 0.3 | 52 ± 1.2 | 13.4 ± 0.5 | 51 ± 2 | 14 ± 3 | 37 ± 3 |
| mica | 2 | *b* | *b* | 14.9 ± 0.5 | 56 ± 2 | 37 ± 8 | 19 ± 8 |

[a] The solution age denotes the time delay between preparation of the solution and immersion of the substrate. The AFM images of the corresponding samples are shown in Figure 4. The partial surface coverages of ordered ($\Theta_{Po}$) and disordered ($\Theta_{pd}$) portions of the submonolayer films are based on the total AFM coverages $\Theta_{AFM}$ and were derived from the IR spectra shown in Figure 5. See text for details. [b] Not determinable by ellipsometry. [c] Insufficient signal-to-noise ratio in the IR spectra.

2 h old solutions were used for IR measurements. On silicon (Figure 5A), the same spectral fitting procedure as described in the previous section was applied, yielding a ratio of about 1:3.5 between ordered and disordered regions for a total surface coverage of 50%. On mica (Figure 5B), which is not suitable for IR reflection spectroscopy, an IR transmission spectrum of

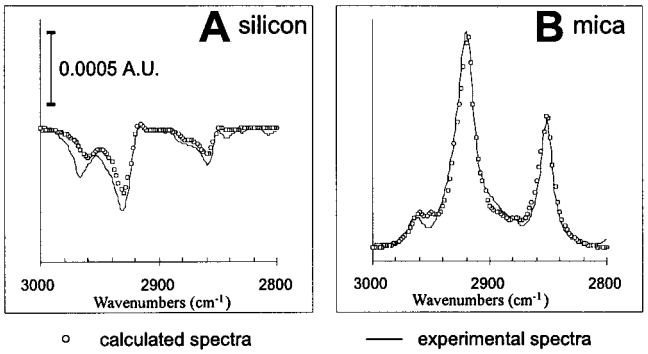


**Figure 5.** CH stretching absorptions of submonolayer ODS films in an IR reflection spectrum on native silicon (A) and in an IR transmission spectrum on mica (B). Both samples were prepared by immersing the substrates for 20 s in the adsorbate solution 2 h after solution preparation. The corresponding AFM images and height profiles are shown in the bottom part of Figure 4.

the submonolayer film at oblique incidence (see Experimental Section) was measured and treated in the same way as a mixture between a crystalline, ordered monolayer structure and a liquidlike, disordered film structure in the spectral fitting procedure. Although a very good agreement between the experimental and simulated spectrum in Figure 5B is achieved for a total surface coverage of 56% and a ratio of 2:1 between ordered and disordered film regions, the experimental error of these data derived from IR transmission spectra is significantly larger (Table 2) as compared to the external reflection spectra on silicon for the following reasons: In the transmission mode, the absorptions of both a disordered, isotropic film and an oriented, anisotropic monolayer point in the same direction and differ by just a few wavenumbers in their peak frequencies and half-widths. A superposition of these very similar transmission spectra, which results in a sum spectrum with some intermediate peak frequencies, is intrinsically less sensitive to the ratio of isotropic and anisotropic contributions as compared to reflection spectra on silicon, where the isotropic and anisotropic absorptions (at least the major $\nu(CH_2)$ bands) point in opposite directions, resulting in the typical differential band profiles shown in Figures 2 and 5A. Additionally, small errors in the spectral parameters (peak frequencies, intensities, half-widths) of the reference spectra used for the simulations will falsify the resulting partial surface coverages $\Theta_{po}$ and $\Theta_{pd}$ more strongly in a transmission spectrum. Yet, there are two major differences beyond these experimental uncertainties to be noted in Table 2 between silicon and mica: First, the adsorption rate is significantly higher on mica—the total surface coverages (Table 2) are 23% (fresh solution) and 56% (2 h old solution) on mica as compared to 4% and 50% on silicon for identical experimental conditions. Second, the ratio $\Theta_{po}/\Theta_{pd}$ shifts from about 1:3.5 on silicon to 2:1 on mica, i.e., the ordered film structure is strongly favored on the mica surface, although this is not accompanied by a corresponding increase of the average island size and/or island height on mica in comparison to silicon (Figure 4). Thus, there is no clear correlation between the degree of structural order derived from IR reflection spectra and the island morphology imaged by AFM, which would allow a localization of ordered and disordered fractions in the AFM images. This indicates, as we have pointed out before, that the real film structure is certainly a lot more complex than assumed in the simplistic model for the IR spectra simulations. The coexistence of different structural domains, which is clearly evident in the experimental IR spectra, does not exclude subtle structural transitions within each domain, resulting in certain

distributions for the chain tilt angle, the packing intensity, or the island height with no predefined thresholds to mark the border between ordered and disordered domains. Even the large, well-ordered islands in Figures 1B or 3B, for example, will contain disordered regions—preferably at the island edges—with a smaller local thickness, lower packing density, and higher conformational disorder. The limiting values for these structural parameters corresponding to either a perfectly ordered phase or a completely disordered state, which form the basis for the IR spectral simulations, are therefore approached but never fully reached in the real film structure.

## Conclusions

A major finding of this study is the observation that both a continuous growth (formation of disordered, liquidlike submonolayer species) and an island-type growth (formation of organized aggregates with vertically aligned hydrocarbon chains) are involved in the formation of ODS monolayers, whose relative contributions depend strongly on the experimental parameters used for film preparation (see below). The following qualitative trends can be derived from the data presented in Table 1: In the early stages of the adsorption process, continuous growth dominates and leads to some intermediate, maximum coverage of disordered film molecules whereas island-type growth is comparatively slow in this region. At intermediate coverages, the surface concentration of disordered species decreases again, accompanied by a sharp increase of ordered island structures on the surface. Since the adsorption of silanol monomers or oligomers as the active precursors in this process is essentially irreversible,[7] this decrease of disordered film molecules must be ascribed to their conversion into larger, ordered aggregates by surface diffusion. Additionally, there is still sufficient empty space on the surface to allow for the deposition of larger, preordered aggregates from solution. Thus, two different processes (surface diffusion and adsorption from solution) contribute to the formation of ordered islands at intermediate coverages, which accounts for the rapid increase of structural order in this range. Finally, at high surface coverage, the remaining surface sites are slowly filled up, presumably by monomeric or small oligomeric species, whose size must be compatible with the small holes in the almost complete monolayer film.

Further support for this model of competitive growth of disordered film domains and oriented island structures comes from the observed influence of certain solution properties (water concentration, solution age) on the growth process. First of all, increasing the water concentration in solution increases the overall growth rate in accordance with previous results.[5,38] Under the reasonable assumption that the composition of the substrate surface does not change within the small range of water concentrations applied in the present study, this growth rate increase must be ascribed to an increase in the silanol concentration in solution, caused by either a shift in the equilibrium concentrations or a rate increase of the hydrolysis reaction $RSiCl_3 + 3H_2O \rightarrow RSi(OH)_3 + 3HCl$. The latter kinetic interpretation is strongly favored by our observation that the film growth rate increases not only with the water concentration but also with the age of the adsorbate solution. Using the same argumentation, we can interpret the observed shift toward an island-type growth mechanism with increasing water concentration in a similar way: It is well-known that the hydrolysis of long-chain alkylchlorosilanes is an exceedingly complex reaction, yielding various kinds of oligomeric and polymeric condensation products[39] as well as surfactant-like microphases consisting of highly organized assemblies of monomeric or partially cross-linked silanol molecules.[40] The specific types, concentrations, and formation rates of these species formed in solution depend on a number of parameters including temperature, precursor concentration, water concentration, and type of solvent, whose influence is only qualitatively understood today. Increasing the water concentration, for example, is known to shift the species distribution toward higher molecular weight products and leads, ultimately, to a deposition of insoluble polymers, which exhibit little chain organization due to an extensive, random cross-linking via Si−O−Si bridges.[40] Allara et al.[40] have shown recently, however, that Si−O−Si polymerization can be largely supressed under certain experimental conditions and highly ordered, layered polymers can be isolated in which the hydrocarbon chains show the same dense and uniform packing as in self-assembled monolayers. The critical role of water in the formation of such ordered phases is demonstrated in these layered polymers by the intercalation of one monolayer of water sandwiched between two layers of alkylsiloxane molecules. On the basis of these results, we speculate that an increase of the water concentration in the adsorbate solution favors the formation and adsorption of such larger, preordered assemblies and shifts the film formation toward an island-type growth process. Our observation that the solution age has again a similar effect as the water concentration indicates that the formation of such macromolecular assemblies in solution is, in part, kinetically controlled within the typical time scale of the monolayer growth.

Finally, we have observed two significant differences in the film growth on silicon and mica substrates. Under identical experimental conditions, the adsorption rate is always higher—particularly in the low-surface coverage region—on mica as compared to silicon, which indicates some additional activation of the mica surface with respect to silanol adsorption. It is known that the cleavage plane of muscovite mica contains potassium ions, which are usually hydrated by atmospheric water and also dissolve to a certain extent in an ambient solvent, leaving negative surface charges behind.[41,42] This might cause an additional, electrostatic attraction of the silanol molecules via their slightly acidic hydrogen atoms and give rise to an enhanced adsorption rate as compared to a neutral surface such as native silicon. The second difference refers to the shape of the submonolayer islands in the AFM images. On mica, submonolayer deposits tend to already coalesce at low surface coverages and form smooth, "brain-like" structures (see the bottom image of Figure 4 for a typical example), whereas on silicon, isolated features of different size and shape persist up to fairly high coverages. This observation points to a higher surface mobility of the silanol species on a mica surface, where the hydroxyl group concentration is much smaller in comparison to silicon and the chances for the film molecules to get trapped and covalently linked to the surface are greatly reduced. This would also explain the observed higher degree of structural order for submonolayer films on mica as compared to silicon for a similar total surface coverage (Table 2). Further studies are currently in progress in our laboratory to quantify the film growth kinetics and the relative contributions of island growth and continuous growth as a function of various solution properties (type of solvent, water content, solution age, temperature) and to elaborate on the influence of the substrate using a combination of different methods (AFM, IR-ATR, ellipsometry) in an in situ configuration.

**Acknowledgment.** This work was supported by the Fonds zur Förderung der Wissenschaftlichen Forschung (Project No. P 9749) and the Hochschuljubiläumsstiftung der Stadt Wien.

## References and Notes

(1) Sagiv, J. *J. Am. Chem. Soc*. **1980**, *102*, 92−98.
(2) Ulman, A. *Chem. Rev*. **1996**, *96*, 1533−1554.
(3) Guyot-Sionnest, P.; Superfine, R.; Hunt, J. H.; Shen, Y. R. *Chem. Phys. Lett*. **1988**, *144*, 1−5.
(4) Tillman, N.; Ulman, A.; Schildkraut, J. S.; Penner, T. L. *J. Am. Chem. Soc*. **1988**, *110*, 6136−6144.
(5) Wasserman, S. R.; Tao, Y. T.; Whitesides, G. M. *Langmuir* **1989**, *5*, 1074−1087.
(6) Silberzan, P.; Leger, L.; Ausserre, D.; Benattar, J. J. *Langmuir* **1991**, *7*, 1647−1651.
(7) Parikh, A. N.; Allara, D. L.; Azouz, I. B.; Rondolez, F. *J. Phys. Chem*. **1994**, *98*, 7577.
(8) Hoffmann, H.; Mayer, U.; Krischanitz, A. *Langmuir* **1995**, *11*, 1304−1312.
(9) Jeon, N. L.; Finnie, K.; Branshaw, K.; Nuzzo, R. G. *Langmuir* **1997**, *13*, 3382−3391.
(10) Kessel, C. R.; Granick, S. *Langmuir* **1991**, *7*, 532−538.
(11) Schwartz, D. K.; Steinberg, S.; Israelachvili, J.; Zasadzinski, J. A. N. *Phys. Rev. Lett*. **1992**, *69*, 3354−3357.
(12) Peanasky, J.; Schneider, H. M.; Granick, S.; Kessel, C. R. *Langmuir* **1995**, *11*, 953−962.
(13) Gun, J.; Iscovici, R.; Sagiv, J. *J. Colloid Interface Sci*. **1984**, *101*, 201−213.
(14) Maoz, R.; Sagiv, J. *J. Colloid Interface Sci*. **1984**, *100*, 465−496.
(15) Cheng, S. S.; Scherson, D. A.; Sukenik, C. N. *J. Am. Chem. Soc*. **1992**, *114*, 5436.
(16) Brunner, H.; Mayer U.; Hoffmann H. *Appl. Spectrosc*. **1997**, *51*, 209−217.
(17) Banga, R.; Yarwood, J.; Morgan, A. M.; Evans B.; Kells, J. *Langmuir* **1995**, *11*, 4393.
(18) Ohtake, T.; Mino, N.; Ogawa, K. *Langmuir* **1992**, *8*, 2081−2083.
(19) Thompson, W. R.; Pemberton, J. E. *Langmuir* **1995**, *11*, 1720.
(20) Finklea, H. O.; Robinson, L. R.; Blackburn, A.; Richter, B.; Allara, D. L.; Bright, T. *Langmuir* **1986**, *2*, 239.
(21) Allara, D. L.; Parikh, A. N.; Rondolez, F. *Langmuir* **1995**, *11*, 2357−2360.
(22) Wasserman, S. R.; Whitesides, G. M.; Tidswell, I. M.; Ocko, B. M.; Pershan, P. S.; Axe, J. D. *J. Am. Chem. Soc*. **1989**, *111*, 5852−5861.
(23) Angst, A. L.; Simmons, G. W. *Langmuir* **1991**, *7*, 2236−2242.
(24) Banga, R.; Yarwood, J.; Morgan, A. M. *Langmuir* **1995**, *11*, 618.
(25) Tidswell, I. M.; Rabedeau, T. A.; Pershan, P. S.; Kosowsky, S. D.; Folkers, J. P.; Whitesides, G. M. *J. Chem. Phys*. **1991**, *95*, 2854−2861.
(26) Bierbaum, K.; Grunze, M.; Baski, A. A.; Chi, L. F.; Schrepp, W.; Fuchs, H. *Langmuir* **1995**, *11*, 2143−2150.
(27) Gauthier, S.; Aime, J. P.; Bouhacina, T.; Attias, A. J.; Desbat, B. *Langmuir* **1996**, *12*, 5126−5137.
(28) Carson, G. A.; Granick S. *J. Mater. Res*. **1990**, *5*, 1745−1751.
(29) Woodward, J. T.; Doudevski, I.; Sikes, H. D.; Schwartz, D. K. *J. Phys. Chem*. **1997**, *101*, 7535.
(30) McCrackin, F. L.; Passaglia, E.; Stromberg, R. R.; Steinberg, H. L. *J. Res. Natl. Bur. Stand., Sect. A* **1963**, *67*, 363.
(31) *Handbook of Optical Constants of Solid*; Palik, E. D., Ed.; Academic Press: New York, 1985.
(32) Although the refractive index of the adsorbate film is certainly a function of coverage, it is not directly determinable for submonolayer films and is, therefore, commonly assumed to be constant and equal to the value of a full monolayer, which means that any changes in the ellipsometric angles $\Delta$ and $\Psi$ are interpreted as changes in film thickness. The error introduced by this assumption has been shown (see ref 7) to be small (<1 Å) for hydrocarbon films undergoing a transition from a liquidlike structure ($n \approx 1.43$) at low coverage to a crystalline, densely packed structure ($n \approx 1.50$) at high coverage (continuous film growth). For an island-type growth mechanism, on the other hand, the (macroscopic) film refractive index is expected to change more drastically between $n = 1$ (uncovered surface in contact with air) and 1.50 (full monolayer), see ref 22. Whereas the true film thickness (i.e., the height of the islands) is independent of coverage in this case, the ellipsometrically measured values for an assumed constant refractive index represent the weighted average of covered and uncovered surface regions and, therefore, reflect the changes in film *density* rather than changes in film *thickness*.
(33) Hoffmann, H.; Mayer, U.; Brunner, H.; Krischanitz, A. *Vib. Spectrosc*. **1995**, *8*, 151.
(34) Carson, G.; Granick S. *Appl. Spectrosc*. **1989**, *43*, 473−476.
(35) Yen, Y. S.; Wong, J. S. *J. Phys. Chem*. **1989**, *93*, 7208−7216.
(36) Strictly speaking, muscovite mica has biaxial optical properties due to its monoclinic crystal structure and is characterized by three different refractive indices along three mutually perpendicular optical axes. For a certain sample configuration, however, with p-polarized light incident at the Brewster angle, mica exhibits pseudoisotropic optical properties described by a single refractive index, see ref 34.
(37) Brunner, H.; Vallant, T.; Mayer, U.; Hoffmann, H. *Surf. Sci*. **1996**, *368*, 279−291.
(38) Brunner, H.; Gibson, C. A.; Mayer, U.; Hoffmann H. *Microchim. Acta* **1997**, *14*, 625−626.
(39) Baney, R. H.; Itoh, M.; Sakakibara, A.; Suzuki, T. *Chem. Rev*. **1995**, *95*, 1409−1430.
(40) Parikh, A. N.; Schivley, M. A.; Koo, E.; Seshadri, K.; Aurentz, D.; Mueller, K.; Allara, D. L. *J. Am. Chem. Soc*. **1997**, *119*, 3135−3143.
(41) Raussel-Colom, J.; Serratosa, J. In *Chemistry of Clays and Clay Minerals*; Newman, A., Ed.; Wiley: New York, 1985; Chapter 8.
(42) Pashley, A. M. *J. Colloid Interface Sci*. **1981**, *80*, 153.